

The Nuclear Force from Lattice QCD

N. Ishii^{1,2} S. Aoki³ and T. Hatsuda²

¹ Center for Computational Sciences, University of Tsukuba, Tsukuba 305-8577, Ibaraki, JAPAN,

² Department of Physics, University of Tokyo, Tokyo 113-0033, JAPAN, and

³ Graduate School of Pure and Applied Sciences,
University of Tsukuba, Tsukuba 305-8571, Ibaraki, JAPAN

The nucleon-nucleon (NN) potential $V_{NN}(r)$ is studied by the lattice QCD simulations in the quenched approximation, using the plaquette gauge action and the Wilson quark action on a 32^4 ($\simeq (4.4 \text{ fm})^4$) lattice. From the equal-time Bethe-Salpeter wave function, we extract the central part of the NN potentials in the 1S_0 and 3S_1 channels. The extracted potential has a strong repulsive core of a few hundred MeV at short distances ($r \lesssim 0.5 \text{ fm}$) surrounded by a relatively weak attraction at medium and long distances. These features are consistent with the empirical structure of the nuclear force.

PACS numbers: 12.38.Gc, 13.75.Cs, 21.30.Cb

More than 70 years ago, Yukawa introduced the pion to account for the strong interaction between the nucleons (the nuclear force) [1]. Since then, enormous efforts have been devoted to understand the nucleon-nucleon (NN) potential at low energies both from theoretical and experimental points of view.

As shown in Fig.1, the NN potential is thought to be characterized by three distinct regions; the long range, the medium range and the short range parts [2, 3]. The long range part ($r \gtrsim 2 \text{ fm}$) is well understood and is known to be dominated by the pion exchange. The medium range part ($1 \text{ fm} \lesssim r \lesssim 2 \text{ fm}$) receives significant contributions from the exchange of multi-pions and heavy mesons (ρ , ω , and σ). The short range part ($r \lesssim 1 \text{ fm}$) is empirically known to have strong repulsive core [6], which is essential for describing the NN scattering data, for the stability and saturation of atomic nuclei, for determining the maximum mass of neutron stars, and for igniting the Type II supernova explosions [7]. The origin of the repulsive core must be intimately related to the

quark-gluon structure of the nucleon. However, it is not yet understood from QCD and remains as one of the most fundamental problems in nuclear and hadron physics [8].

In this Letter, we report our first successful attempt to attack the nuclear force using lattice QCD simulations [9]. The essential idea is to derive the NN potential from the equal-time Bethe-Salpeter (BS) wave function, which satisfies the effective Schrödinger equation in the non-relativistic regime. This is a generalization of the approach recently proposed by CP-PACS collaboration to study the $\pi\pi$ scattering on the lattice [10, 11]. As we shall see below, we have indeed found a strong repulsive core of about a few hundred MeV at short distances surrounded by a relatively weak attraction at medium and long distances in the s-wave channel of the NN potential.

Let us start with the effective Schrödinger equation obtained from the BS equation for two nucleons after non-relativistic reduction [2, 12]:

$$-\frac{1}{2\mu} \nabla^2 \phi(\vec{r}) + \int d^3 r' U(\vec{r}, \vec{r}') \phi(\vec{r}') = E \phi(\vec{r}), \quad (1)$$

where $\mu \equiv m_N/2$ and E is the reduced mass of the nucleon and the non-relativistic energy, respectively. In general, the non-local kernel U depends on E .

For the two nucleons at low energies, U can be represented by the local potentials as $U(\vec{r}, \vec{r}') = V_{NN}(\vec{r}, \nabla) \delta(\vec{r} - \vec{r}')$ [2]. Also the most general NN potential $V_{NN}(\vec{r}, \nabla)$ is severely constrained by various symmetries and is known to have the form;

$$V_{NN} = V_C(r) + V_T(r) S_{12} + V_{LS}(r) \vec{L} \cdot \vec{S} + O(\nabla^2). \quad (2)$$

Here $S_{12} = 3(\vec{\sigma}_1 \cdot \hat{r})(\vec{\sigma}_2 \cdot \hat{r}) - \vec{\sigma}_1 \cdot \vec{\sigma}_2$ is the tensor operator with $\hat{r} \equiv |\vec{r}|/r$, \vec{S} the total spin operator, and $\vec{L} \equiv -i\vec{r} \times \vec{\nabla}$ the relative angular momentum operator. For the general spin-isospin combination, the central NN potential $V_C(r)$, the tensor potential $V_T(r)$ and the spin-orbit potential $V_{LS}(r)$ can be further decomposed as $V_i(r) = V_i^1(r) + V_i^\sigma(r) \vec{\sigma}_1 \cdot \vec{\sigma}_2 + V_i^\tau(r) \vec{\tau}_1 \cdot \vec{\tau}_2 + V_i^{\sigma\tau}(r) (\vec{\sigma}_1 \cdot \vec{\sigma}_2)(\vec{\tau}_1 \cdot \vec{\tau}_2)$

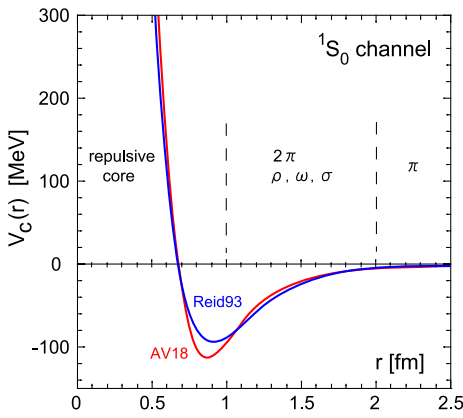


FIG. 1: Two examples of the modern NN potential in the 1S_0 (spin singlet and s-wave) channel. AV18 is from [4] and Reid93 is from [5].

($i = \text{C, T, LS}$). In the phenomenological determination of $V_i(r)$, the Schrödinger equation Eq.(1) with a certain parametrization of $V_i(r)$ in Eq.(2) is solved and compared with the NN phase-shift data [3, 4, 5]. On the other hand, if we can calculate $\phi(\vec{r})$ directly from lattice simulations, Eq.(1) can be used to define the NN potential. Namely, it is *schematically* written as

$$V(\vec{r}) = E + \frac{1}{2\mu} \frac{\vec{\nabla}^2 \phi(\vec{r})}{\phi(\vec{r})}. \quad (3)$$

On the lattice, $\phi(\vec{r})$ with zero angular momentum ($\ell = 0$) is defined from the equal-time BS wave function as

$$\begin{aligned} \phi(\vec{r}) &\equiv \frac{1}{24} \sum_{\mathcal{R} \in O} \frac{1}{L^3} \sum_{\vec{x}} \quad (4) \\ &\times P_{ij}^{\tau} P_{\alpha\beta}^{\sigma} \left\langle 0 \left| N_{\alpha}^i(\mathcal{R}\vec{r} + \vec{x}) N_{\beta}^j(\vec{x}) \right| \text{NN} \right\rangle, \end{aligned}$$

where $N_{\alpha}^i = \epsilon_{abc} ({}^t q^a C \gamma_5 \tau_2 q^b) q_{\alpha}^{i,c}$ is the local interpolating field for the nucleon. a, b and c the color indices, α and β the Dirac indices, i and j the isospin indices, and $C \equiv \gamma_4 \gamma_2$ the charge conjugation matrix. \vec{r} describes the spatial separation between the nucleons. Since we consider the NN scattering at low energies, we take only the upper components of the nucleon interpolating fields. The summation over the vector \vec{x} projects out the state with zero total-momentum. The summation over discrete rotation \mathcal{R} of the cubic group O projects out the A_1^+ representation which contains $\ell = 0$ state and $\ell \geq 4$ states. The former can be singled out by selecting the lowest energy state with the procedure given in Eq.(5). The spin (isospin) projection is carried out by the operator P^{σ} (P^{τ}); for example, $P_{\alpha\beta}^{\sigma} = (\sigma_2)_{\alpha\beta} (= \delta_{\alpha\beta})$ in the spin-singlet (spin-triplet) channel. The renormalization factor Z , which relates the BS wave function on the lattice and that in the continuum, cancels out in the definition of $V(\vec{r})$ in Eq.(3).

In the actual simulations, Eq. (4) is obtained through the four point nucleon correlator,

$$\begin{aligned} F_{\text{NN}}(\vec{x}, \vec{y}, t; t_0) &\equiv \left\langle 0 \left| N_{\alpha}^i(\vec{x}, t) N_{\beta}^j(\vec{y}, t) \bar{\mathcal{J}}_{\text{NN}}(t_0) \right| 0 \right\rangle \\ &= \sum_n A_n \left\langle 0 \left| N_{\alpha}^i(\vec{x}) N_{\beta}^j(\vec{y}) \right| n \right\rangle e^{-E_n(t-t_0)}. \quad (5) \end{aligned}$$

Here $\bar{\mathcal{J}}_{\text{NN}}(t_0)$ is a source term located at $t = t_0$, which produces the nucleons in appropriate quantum numbers with zero total momentum. To enhance the ground state contribution of the NN system, we adopt the wall source, $\mathcal{J}_{\text{NN}}(t_0) = P_{ij}^{\tau} P_{\alpha\beta}^{\sigma} \mathcal{N}_{\alpha}^i(t_0) \mathcal{N}_{\beta}^j(t_0)$, where \mathcal{N} is obtained from N by replacing q by $Q(t_0) = \sum_{\vec{x}} q(\vec{x}, t_0)$. E_n is the energy of the two-nucleon state $|n\rangle$ and $A_n(t_0) \equiv \langle n | \bar{\mathcal{J}}_{\text{NN}}(t_0) | 0 \rangle$. Since the spatial lattice size L^3 is finite, the energy E takes only discrete value. Furthermore, it has a finite shift from the total energy of the non-interacting nucleons $\Delta E = O(1/L^3)$ to be determined

from the simulations [13]. In particular, E for the scattering state may be negative, if there exists attraction.

In this Letter, we focus on the spin-singlet and spin-triplet channels with zero orbital angular momentum. In the standard notation, the former (latter) is called the ${}^{2s+1}\ell_J = {}^1S_0$ ($= {}^3S_1$) channel, where s, l and J denote the total spin, orbital angular momentum, and the total angular momentum of the two nucleons. The 1S_0 is the simplest channel where only the central potential $V_C(r)$ contributes. On the other hand, there arises a mixing between the 3S_1 and 3D_1 channels because of the tensor force $V_T(r)$. In this case, one may define an effective central potential $V_C^{\text{eff}}(r)$; it consists of the bare central potential and the induced central potential by the 3D_1 admixture [2]. The definition in Eq.(3) with $\phi(\vec{r})$ being projected onto 1S_0 (3S_1) is easily shown to give the central potential (the effective central potential).

To calculate $\phi(\vec{r})$, we have carried out simulations on a 32^4 lattice in the quenched approximation. We employ the plaquette gauge action with the gauge coupling $\beta = 5.7$ and the Wilson quark action. The hopping parameters are chosen to be $\kappa = 0.1665$ and 0.1678 which correspond to $m_{\pi}/m_{\rho} = 0.595$ and 0.438 , respectively. The lattice spacing determined from the ρ meson mass is $a^{-1} = 1.44(2)$ GeV ($a \simeq 0.137$ fm) [14], which leads to the physical size of our lattice as (4.4 fm) 4 . In the following, we will show the results for $\kappa = 0.1665$ which corresponds to $m_{\pi} \simeq 0.53$ GeV, $m_{\rho} \simeq 0.89$ GeV and $m_N \simeq 1.34$ GeV. The case for lighter quark masses will be reported elsewhere. We use the global heat-bath algorithm with overrelaxations to generate the gauge configurations. After skipping 3000 sweeps for thermalization, 500 gauge configurations are collected with the interval of 200 sweeps. The Dirichlet (periodic) boundary condition is imposed on the quark fields in the temporal (spatial) direction. To avoid the boundary effect, the wall source

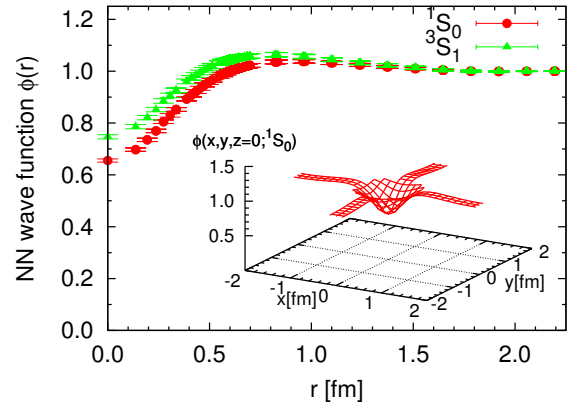


FIG. 2: The lattice QCD result of the radial dependence of the NN wave function at $t-t_0 = 6$ in the 1S_0 and 3S_1 channels. Inset shows the two-dimensional view in the $x - y$ plane.

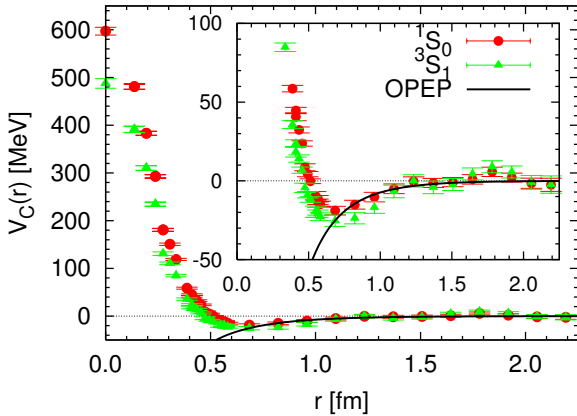


FIG. 3: The lattice QCD result of the central (effective central) part of the NN potential $V_C(r)$ ($V_C^{\text{eff}}(r)$) in the 1S_0 (3S_1) channel for $m_\pi/m_\rho = 0.595$. The inset shows its enlargement. The solid lines correspond to the one-pion exchange potential (OPEP) given in Eq.(6).

is placed at $t = t_0 = 5$ at which the Coulomb gauge fixing is made. The ground state saturation for $t - t_0 \geq 6$ is checked by the effective mass of the two-nucleon system.

Fig. 2 shows the lattice QCD result of the wave function at the time-slice $t - t_0 = 6$. They are normalized at the spatial boundary $\vec{r} = (32/2 = 16, 0, 0)$. All the data including the off-axis ones are plotted for $r \lesssim 0.7$ fm, beyond which we plot only the data locating on the coordinate axes and their nearest neighbors. As is clear from Fig. 2, the wave function is suppressed at short distances and have a slight enhancement at medium distances. This suggests that the NN potential has a repulsion (attraction) at short (medium) distance.

Fig. 3 shows the central (effective central) NN potential in the 1S_0 (3S_1) channel at $t - t_0 = 6$. As for ∇^2 in Eq. (3), we take the discrete form of the Laplacian with the nearest-neighbor points. To obtain the total energy E , the Green's function $G(\vec{r}; E)$ of the Helmholtz equation on the lattice is utilized [10]. By fitting the wave function $\phi(\vec{r})$ at the points $\vec{r} = (10 - 16, 0, 0)$ and $(10 - 16, 1, 0)$ by $G(\vec{r}; E)$, we obtain $E(^1S_0) = -0.49(15)$ MeV and $E(^3S_1) = -0.67(18)$ MeV. This indicates that there is a slight attraction between the two nucleons in a finite box. To check the ground state saturation in terms of the NN potential, we plot the t dependence of $V_C(r)$ in the 1S_0 channel at several distances $r = 0, 0.14, 0.19, 0.69, 1.37$ and 2.19 fm in Fig. 4. We found that the saturation indeed holds for $t - t_0 \geq 6$ within errors.

As anticipated from Fig. 2, both $V_C(r)$ and $V_C^{\text{eff}}(r)$ have repulsive core at $r \lesssim 0.5$ fm with the height of about a few hundred MeV. Also, they have relatively weak attraction of about $-(20-30)$ MeV at the distance $0.5 \lesssim r \lesssim 1.0$ fm. Shown by the solid lines in Fig. 3 are the one-pion exchange contribution to the central poten-

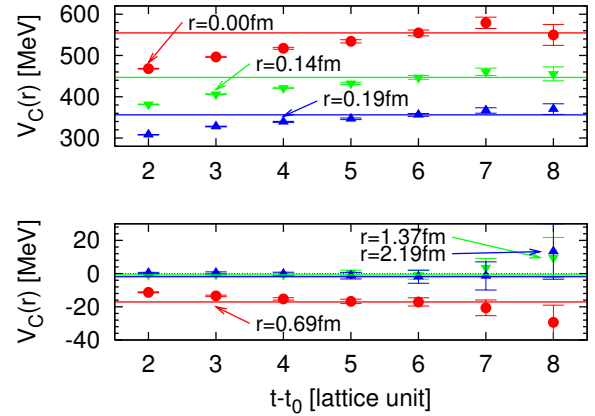


FIG. 4: $t - t_0$ dependence of $V_C(r)$ in the 1S_0 channel for several different values of the distance r .

tial calculated from

$$V_C^\pi(r) = \frac{g_{\pi N}^2}{4\pi} \frac{(\vec{\tau}_1 \cdot \vec{\tau}_2)(\vec{\sigma}_1 \cdot \vec{\sigma}_2)}{3} \left(\frac{m_\pi}{2m_N} \right)^2 \frac{e^{-m_\pi r}}{r}, \quad (6)$$

where we have used the hadron masses corresponding to our data, $m_\pi \simeq 0.53$ GeV and $m_N \simeq 1.34$ GeV, while the πN coupling constant is taken to be the physical value, $g_{\pi N}^2/(4\pi) \simeq 14.0$. One should keep in mind that there is in principle an unphysical ghost contribution in the long-range tail of the NN potential in the quenched approximation. It originates from the flavor-singlet hairpin diagram (the η exchange) between the nucleons [15]. Its contribution to the central potential reads [17]:

$$V_C^\eta(r) = \frac{g_{\eta N}^2}{4\pi} \frac{\vec{\sigma}_1 \cdot \vec{\sigma}_2}{3} \left(\frac{m_\pi}{2m_N} \right)^2 \left(\frac{1}{r} - \frac{m_0^2}{2m_\pi} \right) e^{-m_\pi r}. \quad (7)$$

Here $g_{\eta N}$ and m_0 are the ηN coupling constant and a mass parameter to characterize the ghost, respectively. Eq.(7) has an exponential tail which dominates over the Yukawa potential at large distances. We can estimate its significance by comparing the sign and the magnitude of $e^{m_\pi r} V_C(r)$ and $e^{m_\pi r} V_C^{\text{eff}}(r)$ at large distances, because $V_C^\eta(r)$ has an opposite sign between 1S_0 and 3S_1 . We found no evidence of the ghost contribution in our data at large distances within errors, which may indicate $g_{\eta N} \ll g_{\pi N}$.

Several comments are in order here:

1. Our wave function $\phi(\vec{r})$ provides us with an orthodox way to extract the NN scattering length. According to the standard scattering theory, the asymptotic wave function outside the range of the potential at low energy ($E \rightarrow 0$) is approximated as $\phi^{\text{asy}}(\vec{r}) = \frac{\sin(kr + \delta_0(k))}{kr} \rightarrow \frac{r + a_0}{r}$, where $\delta_0(k)$ is the s-wave scattering phase shift and $a_0 \equiv \lim_{k \rightarrow 0} \delta_0(k)/k$ is the scattering length. By searching the zero of $\phi^{\text{asy}}(\vec{r})$, we find $a_0(^1S_0) = 0.066(22)$ fm and $a_0(^3S_1) = 0.089(27)$ fm under the assumption that $E \sim -0.5$ MeV is small enough

[18]. The reason of having such a small a_0 is easily understood from the well-known formula in the Born approximation: $a_0 \simeq -m_N \int_0^\infty V_C(r) r^2 dr$. It implies that (i) the volume factor $r^2 dr$ hides the repulsive core at short distances, and (ii) a_0 is a subtle quantity obtained as a result of a large cancellation between repulsion and attraction.

2. The above points (i) and (ii) also provide a reason why it is dangerous at the moment to compare a_0 obtained in unphysical quark masses with a_0 in experiments: A slight change of the depth and height of the potential due to the change of the quark mass may affect the scattering length substantially. Indeed, our preliminary results with the lighter quark mass ($m_\pi/m_\rho = 0.438$) shows a tendency that both the short range repulsion and the medium-long range attraction become stronger, which leaves a possibility that $|a_0|$ grows as m_π decreases [16].

3. If the attraction becomes large enough at small m_π , the system may start to have a bound state and the scattering length changes sign from positive to negative. In the real world, this happens in 3S_1 (the deuteron channel). Note that the above mentioned formula in the Born approximation is not valid any more in such a situation. From the inset of Fig. 3, we already see a tendency that the attraction in 3S_1 is stronger than that in 1S_0 . Note that this cannot be attributed to the ghost contribution $(\sigma_1 \cdot \sigma_2) e^{-m_\pi r} / r$ in Eq.(7), because it is repulsive (attractive) in 3S_1 (1S_0).

In summary, we have studied the NN potential by the lattice QCD simulations in the quenched approximation. From the equal-time Bethe-Salpeter wave function of the two-nucleons on a $(4.4 \text{ fm})^4$ lattice with the quark mass corresponding to $m_\pi/m_\rho = 0.595$, the NN potential is extracted via the (non-relativistic) Schrödinger equation. Our way of defining the NN potential on the lattice has direct connection to the empirical NN potential.

The central (effective central) part of the potential in the 1S_0 (3S_1) channel at low energies is found to have a repulsive core at short distances surrounded by a relatively weak attraction at medium and long distances. These properties are known to be most important features of the empirical NN potential. The long range tails of $V_C(r)$ in both channels are not so much different from the one-pion exchange within statistical errors. We did not find numerical evidence of the ghost exchange (quenched artifact) for $m_\pi/m_\rho = 0.595$. Preliminary calculation with the lighter quark mass ($m_\pi/m_\rho = 0.438$) shows a tendency that both the short range repulsion and the medium-long range attraction become stronger.

It would be quite interesting to derive the tensor and spin-orbit forces by making appropriate projections of the wave function. Studies of the hyperon-nucleon and hyperon-hyperon potentials, whose experimental information is currently very limited, are now under investi-

gation: They are particularly important for the physics of hyper nuclei. To unravel the physical origin of the repulsive core, we need further studies on its quark mass dependence, channel dependence, energy dependence, etc. Eventually the full QCD simulations at the physical quark mass are necessary to make a precise comparison of the lattice NN potential to the empirical potentials.

The authors thank N. Ishizuka, U. van Kolck, S. Sasaki and M. Savage for useful comments. N.I. thanks N. Shimizu for useful information and discussions. This research was supported in part by the Grant-in-Aid of MEXT (Nos. 13135204, 15540251, 15540254, 18540253). Our simulations have been performed with IBM Blue Gene/L at KEK under a support of its Large Scale Simulation Program, No.18 and No.06-21 (FY2006).

- [1] H. Yukawa, Proc. Math. Phys. Soc. Japan, **17**, 48 (1935).
- [2] M. Taketani et al., Prog. Theor. Phys. Suppl. **39** (1967), N. Hoshizaki et al., ibid. **42** (1968).
- [3] R. Machleidt and I. Slaus, *J. Phys.* **G27**, R69 (2001).
- [4] R. B. Wiringa, V. G. J. Stoks and R. Schiavilla, *Phys. Rev. C* **51**, 38 (1995).
- [5] V. G. J. Stoks, R. A. M. Klomp, C. P. F. Terheggen and J. J. de Swart, *Phys. Rev. C* **49**, 2950 (1994).
- [6] R. Jastrow, *Phys. Rev.* **81**, 165 (1951).
- [7] R. Tamagaki et al., *Prog. Theor. Phys. Suppl.* **112**, 1 (1993); H. Heiselberg and V. Pandharipande, *Ann. Rev. Nucl. Part. Sci.* **50**, 481 (2000); J. M. Lattimer and M. Prakash, *Phys. Rept.* **333**, 121 (2000).
- [8] F. Myhrer and J. Woldsen, *Rev. Mod. Phys.* **60**, 629 (1988); M. Oka, K. Shimizu and K. Yazaki, *Prog. Theor. Phys. Suppl.* **137**, 1 (2000).
- [9] For a preliminary account on a $(2.2 \text{ fm})^3 \times (3.3 \text{ fm})$ lattice, see N. Ishii, S. Aoki and T. Hatsuda, hep-lat/0610002.
- [10] S. Aoki et al. (CP-PACS Coll.), *Phys. Rev. D* **71** (2005) 094504.
- [11] Our approach is in contrast to the other method where heavy quark(s) must be introduced to define the relative coordinate \vec{r} : D. Arndt, S. R. Beane and M. J. Savage, *Nucl. Phys. A* **726** (2003) 339; T.T. Takahashi, T. Doi and H. Suganuma, hep-lat/0601006.
- [12] R. Machleidt, *Adv. Nucl. Phys.* **19**, 189 (1989).
- [13] M. Lüscher, *Nucl. Phys. B* **354**, 531 (1991).
- [14] M. Fukugita, Y. Kuramashi, M. Okawa, H. Mino, A. Ukawa, *Phys. Rev. D* **52**, 3003 (1995).
- [15] S.R. Beane, M.J. Savage, *Phys. Lett.* **B535**, 177 (2002).
- [16] S.R. Beane, P.F. Bedaque, K. Orginos and M.J. Savage, *Phys. Rev. Lett.* **97**, 012001 (2006).
- [17] If we take into account another ghost parameter α_Φ , the formula is modified as $1/r \rightarrow (1 - \alpha_\Phi)/r$ and $m_0^2 \rightarrow m_0^2 - \alpha_\Phi m_\pi^2$.
- [18] The Lüscher's finite volume formula [13] together with E obtained in the text lead to $a_0(^1S_0) = 0.123(39) \text{ fm}$ and $a_0(^3S_1) = 0.17(5) \text{ fm}$, which are consistent with those obtained from the wave function.